Increased threat of tropical cyclones and coastal flooding to New York City during the anthropogenic era

Andra J. Reed[a,1], Michael E. Mann[a,b], Kerry A. Emanuel[c], Ning Lin[d], Benjamin P. Horton[e,f], Andrew C. Kemp[g], and Jeffrey P. Donnelly[h]

[a]Department of Meteorology, The Pennsylvania State University, University Park, PA 16802; [b]Earth Environmental Systems Institute, The Pennsylvania State University, University Park, PA 16802; [c]Department of Earth, Atmospheric, and Planetary Sciences, Program in Atmospheres, Oceans, and Climate, Massachusetts Institute of Technology, Cambridge, MA 02913; [d]Department of Civil and Environmental Engineering, Princeton University, Princeton, NJ 08544; [e]Department of Marine and Coastal Sciences, Rutgers, The State University of New Jersey, New Brunswick, NJ 08901; [f]Earth Observatory of Singapore and Asian School of the Environment, Nanyang Technological University, Singapore 639798; [g]Department of Earth and Ocean Sciences, Tufts University, Medford, MA 02155; and [h]Department of Geology and Geophysics, Woods Hole Oceanographic Institution, Woods Hole, MA 02543

In a changing climate, future inundation of the United States' Atlantic coast will depend on both storm surges during tropical cyclones and the rising relative sea levels on which those surges occur. However, the observational record of tropical cyclones in the North Atlantic basin is too short (A.D. 1851 to present) to accurately assess long-term trends in storm activity. To overcome this limitation, we use proxy sea level records, and downscale three CMIP5 models to generate large synthetic tropical cyclone data sets for the North Atlantic basin; driving climate conditions span from A.D. 850 to A.D. 2005. We compare pre-anthropogenic era (A.D. 850–1800) and anthropogenic era (A.D.1970–2005) storm surge model results for New York City, exposing links between increased rates of sea level rise and storm flood heights. We find that mean flood heights increased by ~1.24 m (due mainly to sea level rise) from ~A.D. 850 to the anthropogenic era, a result that is significant at the 99% confidence level. Additionally, changes in tropical cyclone characteristics have led to increases in the extremes of the types of storms that create the largest storm surges for New York City. As a result, flood risk has greatly increased for the region; for example, the 500-y return period for a ~2.25-m flood height during the pre-anthropogenic era has decreased to ~24.4 y in the anthropogenic era. Our results indicate the impacts of climate change on coastal inundation, and call for advanced risk management strategies.

tropical cyclones | flood height | storm surge | relative sea level | New Jersey

Tropical cyclones (TCs) and their associated storm surges are the costliest natural hazards to impact the U.S. Atlantic coast (1–3). For example, Hurricane Sandy caused an estimated $50 billion of damage and destroyed at least 650,000 houses in 2012, largely because of flooding from a 3- to 4-m storm surge and large waves (4). A storm surge is the anomalous rise of water above predicted astronomical tides, and its height is driven primarily by wind patterns, storm track, and coastal geomorphology forcing water onshore, with a smaller contribution from reduced atmospheric pressure allowing the ocean surface to rise. The financial cost and human impact of future storm surges will be controlled by the TC climate (frequency, intensity, size, duration, and location) and the rate of relative sea level rise (RSLR), which is the base water level upon which storm surges occur (5, 6). The flood height attained during a given storm is determined by combining storm surge, tides, and relative sea level. Therefore, as sea level rises through time, coastal inundation risk from storm surges rises as well. Thus, it is useful to conduct a long-term analysis of the impact of changing TC climates and RSLR on flood heights (7).

The observational record of TCs in the North Atlantic Ocean basin spans A.D. 1851 to the present, but is too short (8) and potentially unreliable (9) to accurately assess long-term trends in TC frequency, intensity, and storm surge height, particularly for the largest events and for locations that rarely experience landfalling TCs (e.g., refs. 8–13). As an alternative to the observational record of TCs in the North Atlantic Ocean basin, ref. 8 developed a long-term synthetic TC data set, downscaled from the National Center for Atmospheric Research Climate System Model version 1.4 spanning the past millennium, which allows for more accurate assessment of low-frequency variability in TC activity over long periods of time. This process creates a long-term synthetic TC data set consistent with a reasonable past climate (8, 13), and is described in detail in refs. 14 and 15. Here we generate long-term synthetic TC data sets downscaled from the newer, state-of-the-art Coupled Model Intercomparison Project Phase 5 (CMIP5) models. To perform our analysis, we use an interdisciplinary approach that combines TCs with simulated storm surges and proxy relative sea level reconstructions of the last two millennia from southern New Jersey (Fig. 1) (16).

We examine changes in coastal flooding in New York City (NYC) using two time periods to provide a paleoclimate perspective of coastal flooding events such as Hurricane Sandy. We define the anthropogenic era to be a time period in which anthropogenic forcing can be assumed to be dominant (A.D. 1970–2005); we choose the pre-anthropogenic era to be a time period in which anthropogenic forcing can be assumed to be minimal (A.D. 850–1800). Our definition of the end of the time period for the pre-anthropogenic era is consistent with several previous studies (17–19).

Significance

We combine proxy sea level records, downscaled tropical cyclone data sets, and storm surge models to investigate the impacts of rising sea levels and tropical cyclones on coastal inundation in New York City. The flood risk for New York City due to tropical cyclones and their resultant storm surges has increased significantly during the last millennium. Mean flood heights increased by >1.2 m from ~A.D. 850 to A.D. 2005 due to rising relative sea levels. Additionally, there were increases in the types of tropical cyclones that produce the greatest surges for the region. Subsequently, the 500-y flood height return periods have fallen to ~24.4 y throughout the millennium.
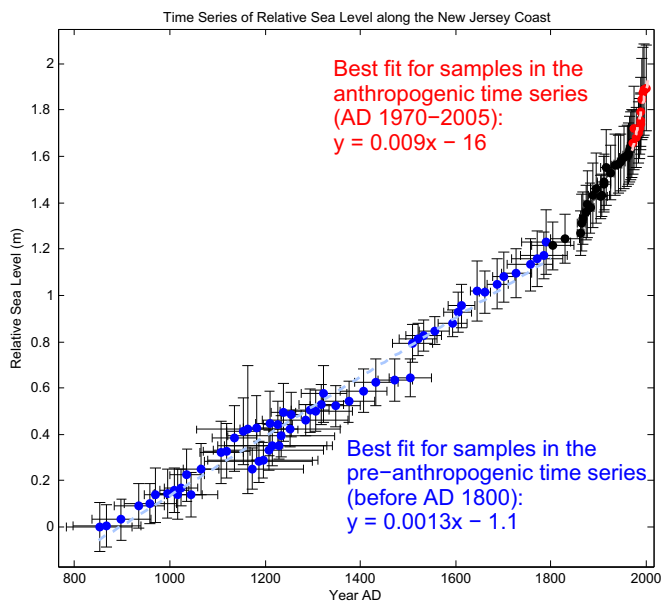
Fig. 1. Relative sea level reconstruction compiled for southern New Jersey using reconstructions from two sites [Leeds Point and Cape May Courthouse (6)]. Samples dated from the pre-anthropogenic era are shown in blue. Samples shown in black are from the interim time period between the pre-anthropogenic and anthropogenic time periods. Samples dated from the anthropogenic era are shown in red. A light blue dashed line shows the best fit line for the pre-anthropogenic era data, and a pink dashed line shows the best fit line for the anthropogenic era data. Equations of the best fit lines are given on the figure. Horizontal error bars represent the 2σ uncertainty, in calendar years, of the year associated with each point. Vertical error bars represent the approximate 1σ uncertainty, in meters, of the sea level associated with each point.

Results

Flood Heights in New York City. To estimate the effect of RSLR on flood heights in NYC since A.D. 850, we combined reconstructed relative sea level with the peak storm surge height for each synthetic storm. The time series in Fig. 1 shows RSLR during the last millennium from proxy reconstructions obtained from southern New Jersey (Fig. 2), with sea levels relative to the sea level in A.D. 852 (16). The accelerated rate of RSLR during the anthropogenic time period (more than 6 times greater than that during the pre-anthropogenic time period) serves as motivation to compare the impacts of RSLR on flood heights during the anthropogenic era to the impacts of RSLR on flood heights during the pre-anthropogenic era for NYC.

Relative sea level for each year was determined using our relative sea level time series, and was added to each of the simulated surge heights at The Battery for the storms from each of our three CMIP5 models (Fig. 3). Nonlinear interaction between RSLR and storm surge was shown to be very small for coastal areas of NYC, using numerical modeling for a range of RSLR up to 1.8 m (20). Additionally, the effect of wave setup for the region is expected to be small (20). Here we focus instead on the evolving variables of RSLR and storm surge. We assume that the influence of changing physiographic conditions is minimal during low rates of RSLR, and thus assume a constant bathymetry and bed roughness during the last millennium (21, 22).

Fig. 3 shows two flood height distributions each for (Fig. 3A) the Max Planck Institute (MPI) Earth System Model, (Fig. 3B) the Coupled Climate System Model 4.0 (CCSM4), and (Fig. 3C) the Institut Pierre Simon Laplace (IPSL) Earth System Model. The means of the anthropogenic distributions of flood height for all three models are ~1.24 m greater than their pre-anthropogenic

counterparts, primarily due to RSLR; this result is significant at the 99% confidence level for each model.

These intuitive results stress the increasing risk that coastal regions of the United States face due to the combination of RSLR and storm surges produced by TCs (22). This risk is amplified in NYC, where the rate of RSLR is greater than the global average due to contributions from regional-scale processes such as glacio-isostatic adjustment (GIA) (23–25). Regardless of uncertainty about the frequency, magnitudes, or tracks of future TCs, risk of coastal inundation for this region will increase as RSLR accelerates. However, it is possible that the risk of higher flood heights due to RSLR could be amplified or dampened by changing climatology of TCs and their resultant storm surges. To better understand this risk, it is necessary to separate the effects of RSLR from changing storm surge height, which results from the prevailing TC climatology.

Changing Storm Surge Heights and Tropical Cyclone Characteristics from the Pre-anthropogenic Era to the Anthropogenic Era. To analyze the impact of changing TC characteristics on flood height, we now neglect the contribution of RSLR to flood height, focusing only on changing storm surge heights. Fig. 4 shows the storm surge height distributions for (Fig. 4A) the MPI model, (Fig. 4B) the CCSM4 model, and (Fig. 4C) the IPSL model. The means of the storm surge height distributions from the pre-anthropogenic and anthropogenic time periods are not statistically different from one another in any of our models.

However, similar to refs. 20 and 26, we find that the storm surge height distributions yielded by our long-term synthetic TC data sets for NYC exhibit long tails. The large but rare events that make up these tails are an important component of determining and planning for the risk of coastal flooding in the NYC region because they are likely to result in the greatest impacts (27). Thus, although the means of the pre-anthropogenic and anthropogenic era storm surge height distributions are not statistically different from one another, it is possible that the frequency of extreme storm surge events, and therefore, the risk of coastal inundation, differs between the two time periods.
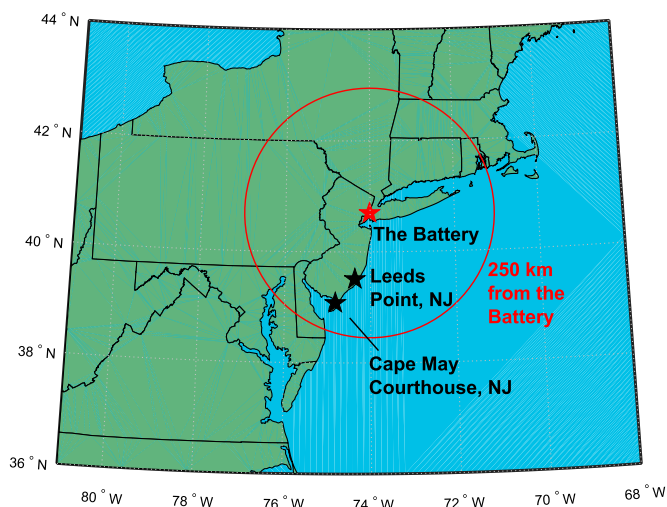

Fig. 2. Map showing the New York and New Jersey coastal region. A filter was used to select storms that moved within 250 km of The Battery in NYC and had maximum winds of at least 40 kts. The Battery is labeled and shown by the red star on the map; a 250-km radius around The Battery is shown by the red circle on the map. Proxy sea level records were constructed from samples obtained at Leeds Point, NJ, and Cape May Courthouse, NJ; both of these locations are labeled and shown by the black stars on the map.
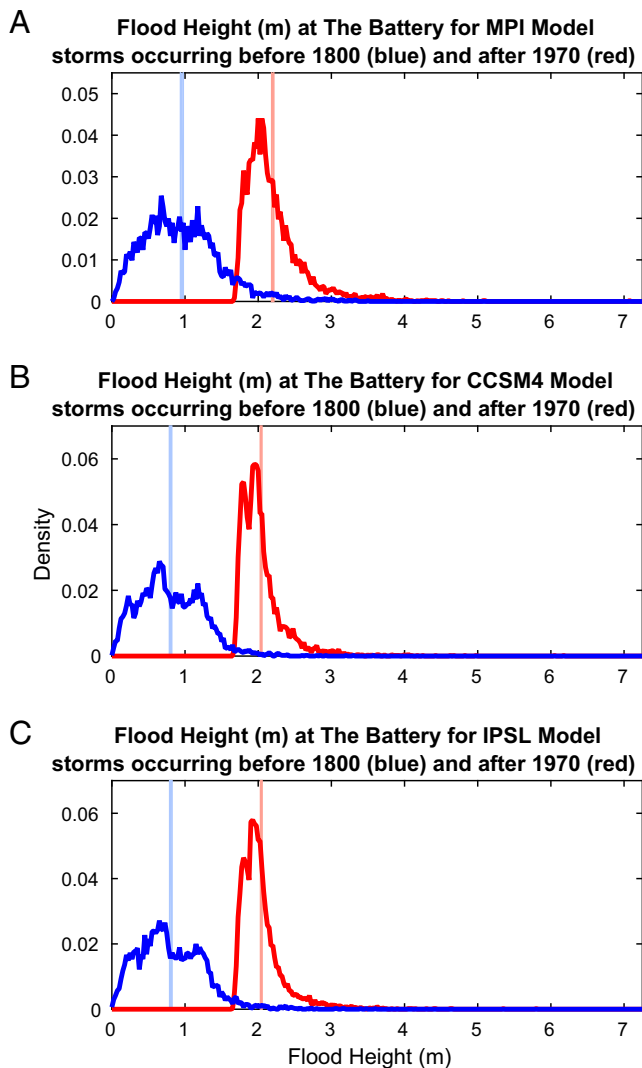
A Flood Height (m) at The Battery for MPI Model storms occurring before 1800 (blue) and after 1970 (red)

B Flood Height (m) at The Battery for CCSM4 Model storms occurring before 1800 (blue) and after 1970 (red)

C Flood Height (m) at The Battery for IPSL Model storms occurring before 1800 (blue) and after 1970 (red)

Fig. 3. Distributions of flood heights for the pre-anthropogenic era (blue) and the anthropogenic era (red) for (*A*) the MPI model, (*B*) the CCSM4 model, and (*C*) the IPSL model. Each distribution is normalized by the number of events it contains. The 99% confidence interval, found by running 100,000 bootstraps of the mean of each set, is shown in light blue for pre-anthropogenic era flood events, and in light red for anthropogenic era flood events.

To investigate differences in the tails of the storm surge height distributions from the two time periods for each model, we created quantile−quantile (Q−Q) plots, in which the quantiles of the normalized, pre-anthropogenic era storm surge distribution are plotted against their counterparts from the normalized anthropogenic era storm surge distribution for each model (Fig. 5 *A*−*C*). Storm surge heights in the tails of the anthropogenic distributions are significantly higher than those in the tails of the pre-anthropogenic distributions for all three models (Fig. 5 *A*−*C*). This indicates that the risk of extreme storm surges is greater in the anthropogenic era than in the pre-anthropogenic era for NYC.

The possible reasons for the larger extreme storm surges in the anthropogenic era were explored using Q−Q plots for several characteristics of the synthetic TCs at the time of landfall for each storm. Fig. 5 *D*−*F* illustrates that tail values in the anthropogenic distributions of radius of maximum winds (RMW) for the synthetic TCs are consistently larger across all three models than

their pre-anthropogenic counterparts. Additionally, Fig. 5 *G*−*L* shows that storms in the tails of the anthropogenic era distributions have lower minimum pressures and higher maximum winds than storms in the tails of the pre-anthropogenic era distributions in all three models. Furthermore, analysis of TC return periods by category illustrates that strong storms (category 3 or greater) tend to have shorter return periods in the anthropogenic era than in the pre-anthropogenic era for all of the models considered here, with the exception of category 5 storms in the IPSL model (Fig. 6). The increase in the frequency of strong storms in NYC during the anthropogenic era corresponds to the increase in storm surge heights during the same time period. For example, we find that for an average flood height of ∼2.25 m, our models had a return period of ∼500 y during the pre-anthropogenic era; the return period for this same flood height has been reduced to ∼24.4 y in the anthropogenic era.

Types of TCs That Produce Flooding in New York City. Furthering our analysis of TC characteristics, we investigate the relationship between storm surge heights and TC intensity and size. Extreme
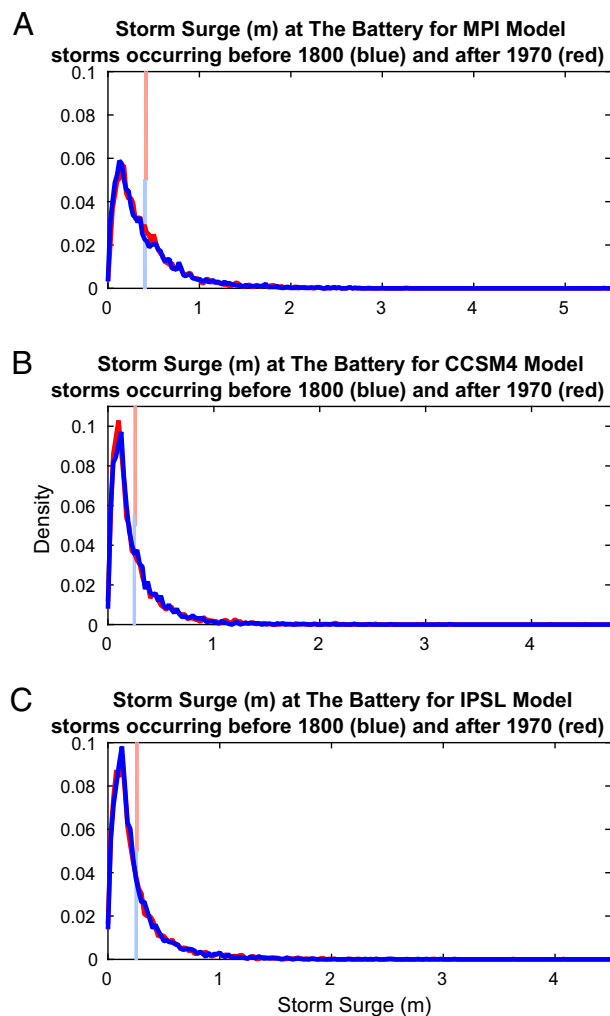

A Storm Surge (m) at The Battery for MPI Model storms occurring before 1800 (blue) and after 1970 (red)

B Storm Surge (m) at The Battery for CCSM4 Model storms occurring before 1800 (blue) and after 1970 (red)

C Storm Surge (m) at The Battery for IPSL Model storms occurring before 1800 (blue) and after 1970 (red)

Fig. 4. Distributions of storm surge heights for the pre-anthropogenic era (blue) and the anthropogenic era (red) for (*A*) the MPI model, (*B*) the CCSM4 model, and (*C*) the IPSL model. Each distribution is normalized by the number of events it contains. The 99% confidence interval, found by running 100,000 bootstraps of the mean of each set, is shown in light blue for pre-anthropogenic era storm surge events, and in light red for anthropogenic era storm surge events.
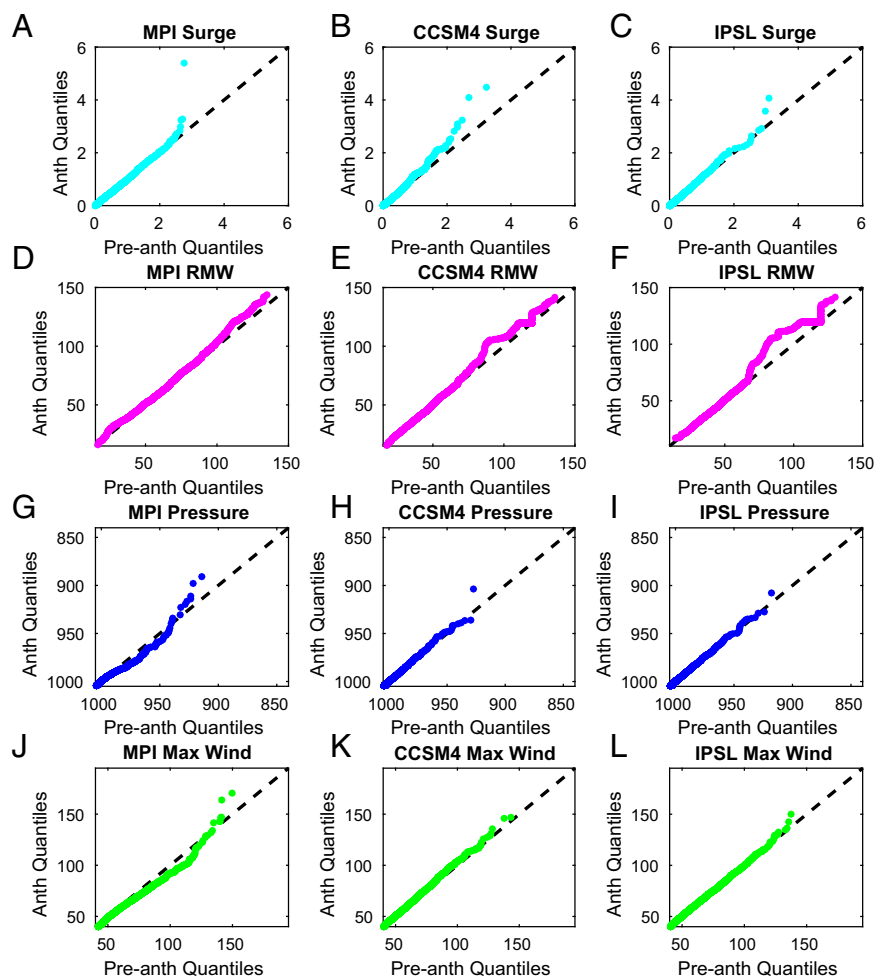
Fig. 5. Q–Q plots indicating differences between the pre-anthropogenic era and anthropogenic era (*A–C*) storm surge heights, (*D–F*) RMW for storms, (*G–I*) minimum storm pressure, and (*J–L*) maximum winds for storms. Results are shown for MPI (*A, D, G,* and *J*), CCSM4 (*B, E, H,* and *K*), and IPSL (*C, F, I,* and *L*) models, and variables are considered at landfall. Dashed lines in the plots indicate the line *y = x*. Points that deviate from this line indicate that the two distributions being compared differ from one another.

surges are often produced by intense storms with strong winds and low pressures. However, an increase in storm surge heights may also be caused by an increase in the storms' RMW [although the intensity and RMW tend not to increase together for individual storms, as there tends to be an inverse relationship between these two quantities (28, 29)]. To further investigate how the storm surges vary with storm characteristics, we perform a principle component analysis (PCA) on the TC characteristics (RMW, storm minimum pressure, and storm maximum winds; Table S1) at landfall that our work identified as likely having an impact on storm surge heights. The PCA indicated that >97% of variance in surge heights across our two time periods and in all three models was described by two main types of storms.

The first type of storm (accounting for more than 80% of the variance in all models) is characterized by large RMW, relatively low wind speeds, and nonextreme minimum pressures. We know from the observational record that large storms with relatively low intensity, such as those that have undergone extratropical transition, can induce large, long-lived surges at The Battery in NYC (30). Hurricane Sandy of 2012 is an example of this type of storm.

When Sandy made landfall in southern New Jersey, it had maximum winds of only ~70 knots (kts), but was a very large [tropical storm force winds extending about 870 nautical miles (4)] and slow-moving storm, capable of producing storm surge

for an extended period in NYC (31). The hazard posed by storms of this type is amplified, because their long-duration storm surges have an increased likelihood of overlapping with a high astronomical tide to produce correspondingly larger flood heights. The current great diurnal tidal range at The Battery is 1.54 m, indicating that the timing of a storm surge is a key control on the flood height attained during a TC event (6). Additionally, ref. 7 indicated that changing thermodynamic conditions could ultimately contribute to stronger versions of large storms like Hurricane Sandy, further increasing the risk of coastal inundation from this type of storm.

The second type of storm (accounting for 10–17% of the variance in storm surge heights in all models) is characterized by smaller RMW, high wind speeds, and low pressures. These relatively intense storms also produce large surges (32).

The Hurricane of 1938 is a historic example of this type of storm impacting the region around NYC. At landfall, this TC was fast-moving (~40 kts), had maximum sustained winds of ~105 kts, and a minimum pressure of ~941 millibars (33). The TC generated a flood height of 1.57 m at The Battery in NYC (6) and a peak flood height of more than 3 m in Long Island, NY (34).

Conclusions

We adopted an interdisciplinary approach that uses proxy relative sea level reconstructions, downscaled synthetic TC data sets,

A MPI Return Period of Storms

B CCSM4 Return Period of Storms

C IPSL Return Period of Storms

Return Period of Storms in Pre-anthropogenic Era

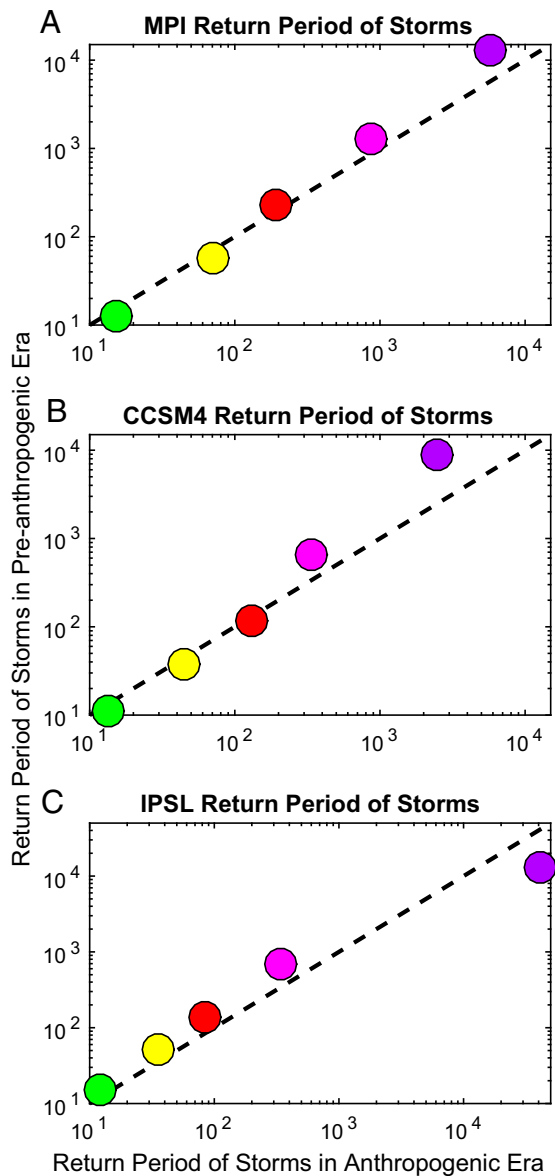Return Period of Storms in Anthropogenic Era

Fig. 6. Comparison of the return periods of storms for the NYC region, by category, in the pre-anthropogenic era (A.D. 850–1800) to the return periods of storms, by category, in the anthropogenic era for (*A*) the MPI model, (*B*) the CCSM4 model, and (*C*) the IPSL model. Categories are according to the Saffir–Simpson scale: Category 1(green), winds 64–82 kts, or 74–95 mph; Category 2 (yellow), winds 83–95 kts, or 96–110 mph; Category 3 (red), winds 96–112 kts, or 111–129 mph; Category 4 (magenta), winds 113–136 kts, or 130–156 mph; Category 5 (purple), winds 137 kts or higher, or 157 mph or higher.

and storm surge models to investigate the impacts of RSLR and TC characteristics on flood heights for NYC. Our results indicate that, compared with the pre-anthropogenic era, flood heights have increased during the anthropogenic era not only due to RSLR but also due to changes in TC characteristics, leading to an increased risk of coastal inundation for NYC. These results indicate the impacts of climate change on coastal inundation, and the necessity for risk management solutions in this highly populated region.

When combining RSLR from our proxy sea level record with storm surges generated by storm surge models for our synthetic TCs, we see that flood heights at The Battery in NYC are significantly greater during the anthropogenic era than during the

pre-anthropogenic era. We find greatly decreased return periods of flood heights across all three of our models when comparing the two time periods. The means of the anthropogenic flood height distributions are statistically greater than the means of the pre-anthropogenic flood height distributions by ∼1.24 m at the 99% confidence level, due to RSLR. Additionally, we find an increased risk of higher surges during the anthropogenic era than during the pre-anthropogenic era for NYC even if RSLR is not considered. Although the means of the pre-anthropogenic and anthropogenic distributions of storm surge heights are not statistically different from one another when RSLR is neglected, the storm surge heights in the tails of the anthropogenic distributions are significantly greater than storm surge heights in the tails of the pre-anthropogenic storm surge distributions.

Our study indicates that during the anthropogenic era, there are increases in the extremes of the types of storms that explain the majority of storm surge for NYC. First, when comparing our two time periods, there is an increase in storm RMW during the anthropogenic era. Although storms with large RMWs may not be particularly intense, they may produce winds capable of creating a storm surge at The Battery for extended periods of time. Additionally, we see more-intense storms with a greater ability to produce high storm surges at The Battery in NYC during the anthropogenic era than during the pre-anthropogenic era.

Methods

Proxy Relative Sea Level Records. We use an existing relative sea level reconstruction from southern New Jersey (16) to describe the long-term baseline on which the simulated storm surges occur. The reconstruction was produced using foraminifera and bulk sediment $\delta^{13}C$ values measured in cores of dated salt marsh sediment from two sites located ∼58 km apart (Cape May Courthouse and Leeds Point; Fig. 2). The Cape May Courthouse record spans the period since ∼A.D. 700, and the Leeds Point record spans the period from ∼500 B.C. to ∼A.D. 1600. Each reconstruction has a 2σ age uncertainty and a 1σ vertical uncertainty. The two reconstructions were combined to produce a single, regional relative sea level record, which is what an observer at the coast would have experienced, and is the net outcome of multiple and simultaneous processes including GIA. A caveat of using this data set is that relative sea level differences between southern New Jersey and NYC may arise over decades to centuries because of spatial differences in the rate of GIA (35), the fingerprint of ice sheet melt (36), and the role of ocean currents, including the strength and position of the Gulf Stream (24, 37).

Relative sea level reconstructions produced from salt marsh sediment do not preserve the seasonal to interannual variability that is evident in tide gauge time series because biological sea level indicators such as foraminifera and plants respond to longer-lived trends and because the slices of sediment used in the reconstruction have a thickness (typically 1 cm) making them time-averaged. Therefore, the proxy reconstruction records multidecadal to centennial-scale relative sea level trends. Seasonal and interannual sea level fluctuations caused by temporary weather patterns (winds and pressure), coastal sea surface temperatures and salinities, and ocean currents can produce fluctuations of up to ∼0.3 m in addition to this trend, as evidenced by the size of annual average relative sea level departures from the overall trend measured at The Battery tide gauge in NYC.

Synthetic Tropical Cyclone Data Sets. We apply the downscaling method developed in refs. 8, 14, and 15 to the MPI, CCSM4, and IPSL CMIP5 models. The downscaling method used by ref. 8 uses monthly mean thermodynamic state variables, including sea surface temperature and vertical profiles of temperature and humidity, as well as daily mean values of interpolated 250-hPa and 850-hPa winds to generate TCs and model their tracks and intensity (8, 14, 15). When modeling the intensity of downscaled TCs, RMW values are also calculated deterministically by the Coupled Hurricane Intensity Prediction System model (15, 38, 39). Our choice of models is dictated by the availability of the necessary thermodynamic and kinematic state variables from A.D. 850–2005, although, for this time period, only the MPI model provides the daily wind fields required for our analysis. In the interest of considering results from more than one model, we use the less desirable monthly values of the wind fields from the CCSM4 and IPSL models, in these cases fixing variances and covariances of winds at the arbitrarily chosen A.D. 1980 values, but allowing the winds to vary over the seasonal cycle (13).

A simple analysis revealed that long-term variations are well-represented by the fixed covariance simulation (e.g., figure 1 in ref. 13).

We require large numbers of TCs to perform a reliable statistical analysis of storm surge heights. Thus, we use a filter to select about 10,000 storms, for each model, that pass within 250 km of The Battery (Fig. 2). Of these storms, ~5,000 were generated in each the pre-anthropogenic and anthropogenic periods. The overall event frequency is calculated from the ratio of the number of TC events simulated to the total number seeded. This ratio is multiplied by a universal calibration constant for each model, derived so as to produce the observed frequency of TCs during the late 20th century (15).

Data used for this project are publicly available from the Earth System Grid Federation website, pcmdi9.llnl.gov/esgf-web-fe/. Researchers interested in downscaled fields may contact coauthor K.A.E. via email with their request.

Storm Surge Modeling. We apply the Advanced Circulation (ADCIRC) model (40) to simulate the storm surges induced by all synthetic storms. ADCIRC is a finite-element hydrodynamic model that has been validated and applied to simulate storm surges and make forecasts for various coastal regions (e.g., refs. 41–44). It uses an unstructured grid with very fine resolution near the coast and much coarser resolution in the deep ocean. The numerical grid we use for this New York/New Jersey region study was created by ref. 20; the grid has a resolution of ~100 m along the NYC coast and was shown to generate results similar to those from a higher-resolution (~10 m) grid (20).

The ADCIRC storm surge modeling is driven by the storm surface wind and pressure fields. Given the characteristics (maximum wind speed, minimum central pressure, and RMW) of the synthetic storms, we estimate the surface wind and pressure fields along the storm track using parametric methods, similar to ref. 20. In particular, the surface wind is estimated by fitting the wind velocity at the gradient height to an analytical hurricane wind profile (45), translating the gradient wind to the surface level with a velocity reduction factor (0.85) and an empirical formula for inflow angles (46), and adding a fraction (0.55 at 20 degrees cyclonically) of the storm translation velocity to account for the asymmetry of the wind field induced by the surface background wind (47). The surface pressure is also estimated from a simple parametric model (48).

1. Emanuel K (2005) Increasing destructiveness of tropical cyclones over the past 30 years. *Nature* 436(7051):686–688.
2. Pielke RA, Jr (2007) Future economic damage from tropical cyclones: sensitivities to societal and climate changes. *Philos Trans R Soc A* 365(1860):2717–2729.
3. Rappaport EN (2014) Fatalities in the United States from Atlantic tropical cyclones: New data and interpretation. *Bull Am Meteorol Soc* 95(3):341–346.
4. Blake ES, Kimberlain TB, Berg RJ, Cangialosi JP, Beven JL, II (2013) *Tropical Cyclone Report: Hurricane Sandy (AL182012), 22–29 October 2012* (Natl Hurricane Cent, Miami).
5. Tebaldi C, Strauss BH, Zervas C (2012) Modelling sea level rise impacts on storm surges along US coasts. *Environ Res Lett* 7(1):021001.
6. Kemp AC, Horton BP (2013) Contribution of relative sea-level rise to historical hurricane flooding in New York City. *J Quat Sci* 28(6):537–541.
7. Lackmann GM (2015) Hurricane Sandy before 1900, and after 2100. *Bull Am Meteorol Soc* 96(4):547–560.
8. Kozar ME, Mann ME, Emanuel KA, Evans JL (2013) Long-term variations of North Atlantic tropical cyclone activity downscaled from a coupled model simulation of the last millennium. *J Geophys Res* 118(24):13383–13392.
9. Landsea CW (2007) Counting Atlantic tropical cyclones back to 1900. *Eos Trans AGU* 88(18):197–208.
10. Chang EKM, Guo Y (2007) Is the number of North Atlantic tropical cyclones significantly underestimated prior to the availability of satellite observations? *Geophys Res Lett* 34(14):L14801.
11. Mann ME, Sabbatelli TA, Neu U (2007) Evidence for a modest undercount bias in early historical Atlantic tropical cyclone counts. *Geophys Res Lett* 34(22):L22707.
12. Lin N, Lane P, Emanuel KA, Sullivan RM, Donnelly JP (2014) Heightened hurricane surge risk in northwest Florida revealed from climatological-hydrodynamic modeling and paleorecord reconstruction. *J Geophys Res* 119(14):8606–8623.
13. Reed AJ, Mann ME, Emanuel KA, Titley DW (2015) An analysis of long-term relationships among count statistics and metrics of synthetic tropical cyclones downscaled from CMIP5 models. *J Geophys Res* 120(15):7506–7519.
14. Emanuel KA, Ravela S, Vivant E, Risi C (2006) A statistical-deterministic approach to hurricane risk assessment. *Bull Am Meteorol Soc* 87(3):299–314.
15. Emanuel KA, Sundararajan R, Williams J (2008) Hurricanes and global warming: Results from downscaling IPCC AR4 simulations. *Bull Am Meteorol Soc* 89(3):347–367.
16. Kemp AC, et al. (2013) Sea-level change during the last 2500 years in New Jersey, USA. *Quat Sci Rev* 81:90–104.
17. Meinshausen M, et al. (2011) The RCP greenhouse gas concentrations and their extensions from 1765 to 2300. *Clim Change* 109(1):213–231.
18. Taylor KE, Stouffer RJ, Meehl GA (2012) An overview of CMIP5 and the experiment design. *Bull Am Meteorol Soc* 93(4):485–498.
19. Intergovernmental Panel on Climate Change (2013) *Climate Change 2013: The Physical Science Basis. Contribution of Working Group I to the Fifth Assessment Report of the Intergovernmental Panel on Climate Change*, eds Stocker TF, et al. (Cambridge Univ Press, Cambridge, UK).
20. Lin N, Emanuel KA, Oppenheimer M, Vanmarcke E (2012) Physically based assessment of hurricane surge threat under climate change. *Nat Clim Chang* 2:462–467.
21. Irish JL, et al. (2010) Potential implications of global warming and barrier island degradation on future hurricane inundation, property damages, and population impacted. *Ocean Coast Manage* 53(10):645–657.
22. Woodruff JD, Irish JL, Camargo SJ (2013) Coastal flooding by tropical cyclones and sea-level rise. *Nature* 504(7478):44–52.
23. Peltier WR (1996) Global sea level rise and glacial isostatic adjustment: an analysis of data from the east coast of North America. *Geophys Res Lett* 23(7):GL00848.
24. Davis JL, Mitrovica JX (1996) Glacial isostatic adjustment and the anomalous tide gauge record of eastern North America. *Nature* 379(6563):331–333.
25. Miller KG, Kopp RE, Horton BP, Browning JV, Kemp AC (2013) A geological perspective on sea-level rise and impacts along the U.S. mid-Atlantic coast. *Earths Future* 1(1):3–18.
26. Lin N, Emanuel KA, Smith JA, Vanmarcke E (2010) Risk assessment of hurricane storm surge for New York City. *J Geophys Res* 115(D18):D18121.
27. Aerts JCJH, Lin N, Botzen W, Emanuel K, de Moel H (2013) Low-probability flood risk modeling for New York City. *Risk Anal* 33(5):772–788.
28. Chavas DR, Emanuel KA (2014) Equilibrium tropical cyclone size in an idealized state of axisymmetric radiative–convective equilibrium. *J Atmos Sci* 71(5):1663–1680.
29. Irish JL, Resio DT, Ratcliff JJ (2008) Influence of storm size on hurricane surge. *J Phys Oceanogr* 38(9):2003–2013.
30. Jones SC, et al. (2003) The extratropical transition of tropical cyclones: Forecast challenges, current understanding, and future directions. *Weather Forecast* 18(6):1052–1092.
31. Brandon CM, Woodruff JD, Donnelly JP, Sullivan RM (2014) How unique was Hurricane Sandy? Sedimentary reconstructions of extreme flooding from New York Harbor. *Sci Rep* 4:7366.
32. Weisberg RH, Zheng L (2006) Hurricane storm surge simulations for Tampa Bay. *Estuaries Coasts* 29(6):899–913.
33. Landsea CW, et al. (2014) A reanalysis of the 1931 to 1943 Atlantic hurricane database. *J Clim* 27(16):6093–6118.
34. Donnelly JP, et al. (2001) 700 yr sedimentary record of intense hurricane landfalls in southern New England. *Geol Soc Am Bull* 113(6):714–727.
35. Engelhart SE, Peltier WR, Horton BP (2011) Holocene relative sea-level changes and glacial isostatic adjustment of the U.S. Atlantic coast. *Geology* 39(8):751–754.
36. Mitrovica JX, et al. (2011) On the robustness of predictions of sea level fingerprints. *Geophys J Int* 187(2):729–742.
37. Yin J, Goddard PB (2013) Oceanic control of sea level rise patterns along the East coast of the United States. *Geophys Res Lett* 40(20):5514–5520.
38. Emanuel KA (1989) The finite-amplitude nature of tropical cyclogenesis. *J Atmos Sci* 46(22):3431–3456.
39. Emanuel KA (1995) The behavior of a simple hurricane model using a convective scheme based on subcloud-layer entropy equilibrium. *J Atmos Sci* 52(22):3959–3968.
40. Luettich RA, Westerink JJ, Scheffner NW (1992) *ADCIRC: An Advanced Three-Dimensional Circulation Model for Shelves, Coasts, and Estuaries, Report 1: Theory and Methodology of ADCRIC-2DDI and ADCIRC-3DL* (US Army Corps Eng. Vicksburg, MS), Tech. Rep. DRP-92-6.
41. Westerink JJ, et al. (2008) A basin- to channel-scale unstructured grid hurricane storm surge model applied to southern Louisiana. *Mon Weather Rev* 136(3):833–864.
42. Colle BA, et al. (2008) New York City's vulnerability to coastal flooding. *Bull Am Meteorol Soc* 89(6):829–841.
43. Lin N, Smith JA, Villarini G, Marchok TP, Baeck ML (2010) Modeling extreme rainfall, winds, and surge from Hurricane Isabel (2003). *Weather Forecast* 25(5):1342–1361.
44. Dietrich JC, et al. (2011) Modeling hurricane waves and storm surge using integrally-coupled, scalable computations. *Coast Eng* 58(1):45–65.
45. Emanuel KA, Rotunno R (2011) Self-stratification of tropical cyclone outflow. Part I: Implications for storm structure. *J Atmos Sci* 68(10):2236–2249.
46. Bretschneider CL (1972) A non-dimensional stationary hurricane wave model. *Proc Offshore Technol Conf* 1:51–68.
47. Lin N, Chavas D (2012) On hurricane parametric wind and applications in storm surge modeling. *J Geophys Res* 117(D9):D09120.
48. Holland GJ (1980) An analytic model of the wind and pressure profiles in hurricanes. *Mon Weather Rev* 108(8):1212–1218.

EARTH, ATMOSPHERIC, AND PLANETARY SCIENCES